

# COMMISSIONING OF THE IOTA PROTON INJECTOR\*

A. Romanov<sup>†</sup>, N. Banerjee, D. Broemmelsiek, K. Carlson, D. Edstrom, J. Jarvis, N. Kuklev, D. MacLean, J. Santucci, T. Thompson, M. Wallbank, J. Wieland, Fermilab, Batavia, IL, USA  
B. Simons, Northern Illinois University, DeKalb, IL, USA

## Abstract

The IOTA Proton Injector (IPI) at the Fermilab Accelerator Science and Technology facility (FAST) is a machine capable of delivering up to 14 mA pulses of protons at 2.5 MeV to the Integrable Optics Test Accelerator (IOTA) ring. Its construction has been completed in the fall of 2025, followed by a successful commissioning run scheduled to conclude at the end of May 2026. It operates alongside the existing electron injector beamline to facilitate further beam physics research and continued development of novel accelerator technologies at the IOTA ring. This report details the current operational profile, known challenges, and future plans for the proton program development at FAST.

## INTRODUCTION

The proton injector for the Integrable Optics Test Accelerator (IOTA) [1], shown in Fig. 1, is an important capability for the research program at FAST/IOTA [2]. IOTA is a research storage ring constructed and operated by Fermilab to study advanced concepts in accelerator physics. During the previous runs the studies at IOTA were performed with electron beams of up to 150 MeV energy, which have negligible space-charge effects. The commissioning of the 2.5 MeV IOTA proton injector with a beam current of 14 mA enabled experiments with intense beams that have strong space-charge tune shifts, constituting 10 – 15 % of the total betatron phase advance in the ring.

## PROTON SOURCE

Positive ions with 50 keV kinetic energy are produced in the duoplasmatron ion source (IS) schematically shown in Fig. 2. The resulting beam consists of three different species,

$p$ ,  $H_2^+$  and  $H_3^+$ , and the proportions depend on the exact configuration of the source. This source was previously used as part of the High Intensity Neutrino Source (HINS) experiment [3], and was subsequently adopted by the FAST facility as it fits the desired beam parameters for proton production in the IPI beamline, as shown in Fig. 3. The ion source (IS) was briefly resurrected on site in the HINS enclosure at the Meson Detector Building (MDB) before being fully disassembled and cleaned. During disassembly, it was noted that the 1.25 mm diameter extraction aperture used with HINS was unusually large for a duoplasmatron source, and it has been replaced with a 0.7 mm diameter aperture.

The duoplasmatron uses a filament as a thermionic emitter to excite a DC plasma discharge in the hydrogen gas. Filaments are prepared on-site. The first step is to spot-weld S-shaped mesh to electrodes. It is important to avoid sharp bends and melting through the mesh. The mesh is then gently cleaned with alcohol, and a mixture of barium, calcium, and strontium carbonates is applied. The original recipe involved isoamyl acetate to assist in binding the mixture to the filament and required a lengthy multistep process in a special chamber to avoid contamination of the main vacuum system with hydrocarbon byproducts. In addition, the results were inconsistent in terms of emission efficiency. The final recipe was simplified significantly and consists of the same mix of three carbonates combined with a small amount of isopropyl alcohol to form a paste-like suspension. This paste is then applied to the surface of the nickel mesh with a brush to form a uniform layer that fills the mesh cells. After the alcohol evaporates at room temperature, the activation process can be performed even inside the proton source. There are two outgassing peaks during the process: one corresponds to water evaporation and occurs around 100 °C, and another corresponds to the transformation of carbonates into oxides, which releases carbon dioxide. A filament prepared with this recipe has been in use since spring 2024 and has been

\* This work was produced by FermiForward Discovery Group, LLC under Contract No. 89243024CSC000002 with the U.S. Department of Energy, Office of Science, Office of High Energy Physics.

<sup>†</sup> aromanov@fnal.gov

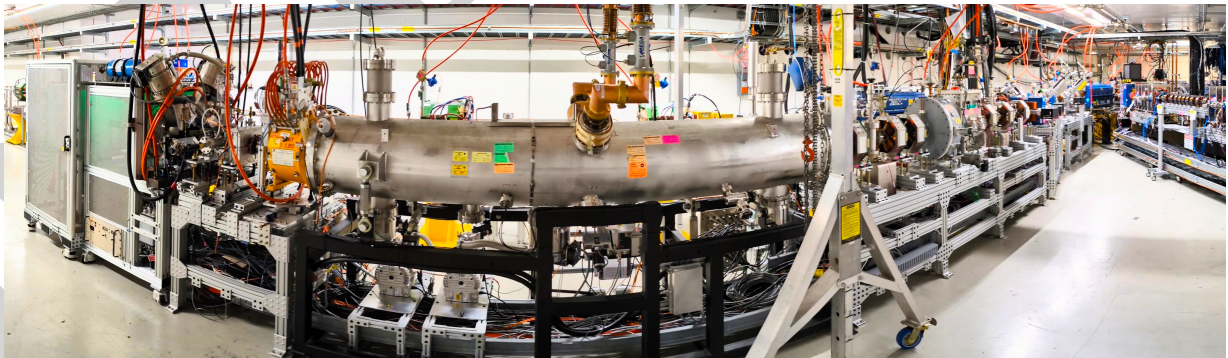


Figure 1: IOTA proton injector.

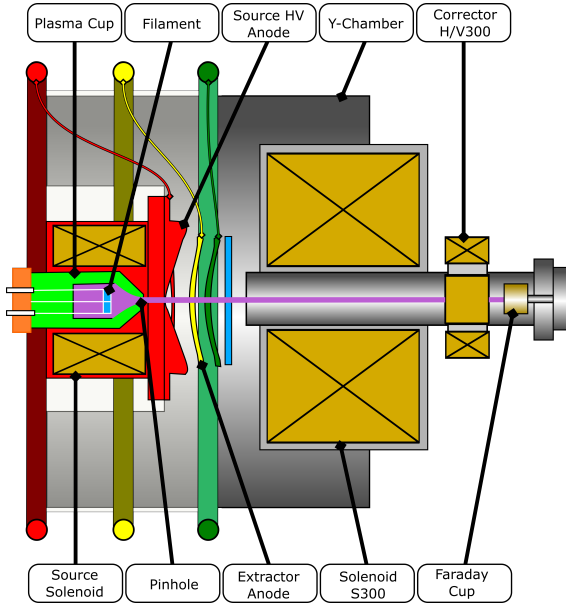


Figure 2: A schematic view of the IS in a test configuration. For extraction of 50 keV protons, the source high voltage anode is charged to a static +50 kV, the extractor anode is set to 40 kV, and the green anode is at ground potential. The S300 solenoid is the first element of the LEBT.

exposed to atmospheric pressure several times with dry nitrogen as a backfill gas. The total number of red-hot hours is 861, and the number of ramps so far is 154.

Before IS installation in the IPI, a short test stub was established in the NML Source Test Cage to study IS output across a range of operational parameters including the plasma cup pressure, extractor and arc amplitudes, and source solenoid current. In some of the configurations the stub included a dipole magnet to act as a spectrometer and two devices, toroid and Faraday cup, to measure beam current. An Allison scanner [4] was also used to measure parameters of the vertical distribution, both for a beam going straight into the scanner and with a spectrometer dipole to separate the species. To help maximize the proton fraction, two slits were added to better isolate different species (Fig. 4). The left plot in Fig. 5 shows beam composition measured before and after optimization. The right plot in Fig. 5 shows a beam scan for total current output, optimized in a different spectrometer configuration with only the aperture of the Faraday cup acting as a selector. Pulses with around 14 mA of protons were produced.

## LEBT

The IPI LEBT, as seen in Fig. 6, is a short section of beamline designed to transport beam from the proton source to the RFQ. The beam envelope is controlled by two solenoids (SOL), and steering is done with two frame trims. Beam diagnostics include two scrapers, a toroid, and an electrically isolated diaphragm (EID). Both the scrapers and the EID can be biased, and their output signals are connected to the control system. It is assumed that, with the assistance of

Table 1: Parameters of the Proton Injector and IOTA with Protons

	Parameter	Nom.	Unit
LEBT	Energy	50	keV
	Proton beam current	14	mA
	Plasma pulse length	80	$\mu$ s
	Extractor pulse length	30	$\mu$ s
	Source pulse rate	1	Hz
MEBT	Energy	2.5	MeV
	RF pulse rate	1	Hz
	RFQ frequency	$325.0 \pm 0.5$	MHz
	Phase stability	1	$^\circ$
	Amplitude stability	1	%
	RFQ duty factor	<0.02	%
	RFQ pulse length	60	$\mu$ s
	Buncher cav. pulse length	60	$\mu$ s
	Bunch length	0.3-1.1	cm
IOTA with protons	Proton beam energy	2.5	MeV
	Relativistic $\beta$	0.0728	
	Circumference	40	m
	Proton RF frequency	30.25 & 2.19	MHz
	Revolution period	1.83	$\mu$ s
	RF voltage	1	kV
	Geometric emittance	3.5	$\mu$ m
	$\Delta p/p$ (RMS)	0.07	%
	Beam current	up to 8	mA
	Momentum compaction	0.07	
Betatron tunes ( $Q_x, Q_y$ )	5.3, 5.3		

the EID, the beam space charge is quickly neutralized by an electron cloud. The beam envelope simulated assuming full neutralization is shown in Fig. 6.

## RFQ

Like the IS, the RFQ was also adopted from the HINS experiment and is tasked with accelerating the proton beam from 50 keV to 2.5 MeV [5, 6]. Due to a cooling-to-vacuum leak [7], it cannot be temperature-regulated. A test performed in 2020 indicates that the net effect will be a  $\sim 5.6$  kHz drop in the resonant frequency over the first 8 hours for an average CW power of  $\sim 100$  W with a tuning loop that kept the cavity on resonance. The average power corresponds to a maximum average power expected with RFQ operation according to the low duty factor cited in Table 1. This test demonstrated a roll-off in frequency drift as the cavity approached thermal equilibrium.

At present the RFQ is operated in an open loop and allowed to drift, but this has not presented significant difficulty to operations. A phase difference between the RFQ and the downstream buncher cavity, taken from the pickup signals between the two, is used to inform the need for any phase adjustment to the downstream cavity, but this too has not caused any immediate operational concern.

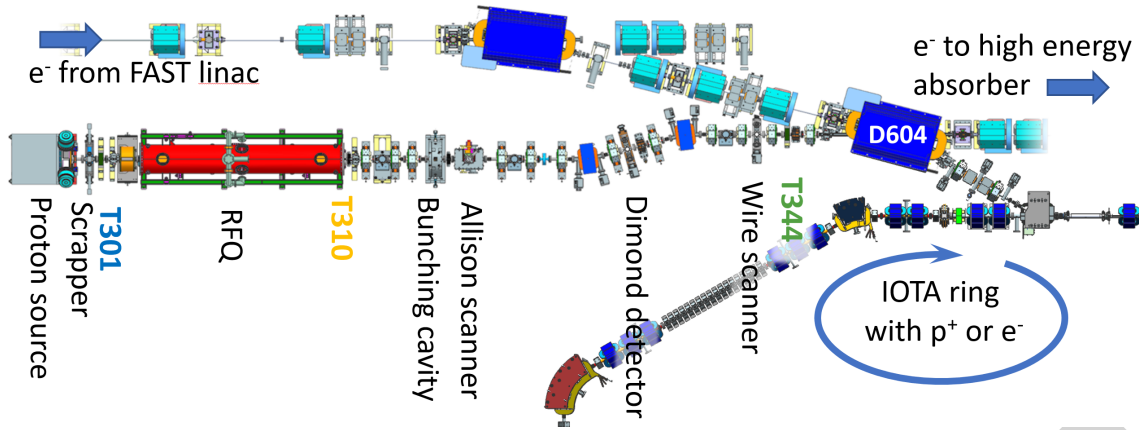


Figure 3: The IPI beamline meets the existing electron injector beamline at the bend dipole D604 and then injects into the IOTA ring along the same trajectory as electrons at 100 to 150 MeV. As such, time must be taken between electron and proton runs in the IOTA ring to allow for the necessary configuration changes.

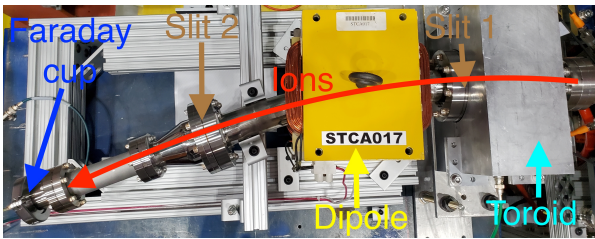


Figure 4: The spectrometer configuration with two narrow slits.

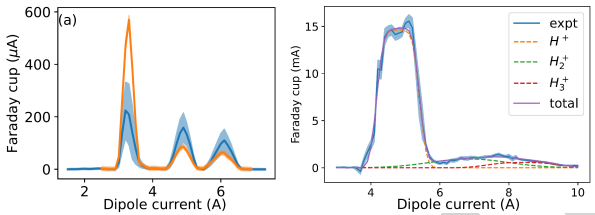


Figure 5: Left: optimization of the protons fraction, blue line is for the initial setup, orange line is optimized proton fraction. Three distinct peaks corresponding to  $p$ ,  $H_2^+$  and  $H_3^+$  are visible with 2 narrow slits in the spectrometer. Right: optimization of the total beam current output with wide open aperture.

### MEBT

The IPI MEBT transports the proton beam from the RFQ through the D604 bend dipole and into IOTA. The section starting from D604 is the existing 300 MeV Electron Injector beamline. During the design stage the beam parameters at the exit of the RFQ were gathered from [6] and later confirmed with simulations [8]. Experimental measurements suggest a factor of two larger normalized emittances of  $6 \mu\text{m}$ . The MEBT includes the bunching RF cavity [9] to reduce the beam momentum spread from about 0.5 % to 0.06 % in a linear approximation. Another important structure in the line is a dogleg that is necessary to excite and match dispersion at the injection point in IOTA. To obtain a fully matched beam while avoiding aperture limitations, a total of 17 quadrupoles are used, including 12 individually powered

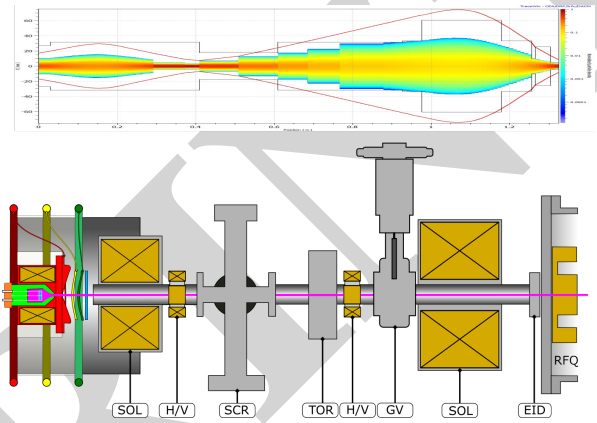


Figure 6: The LEBT configuration and a TraceWin simulation showing aperture restrictions and beam sizes and density through the LEBT.

electromagnets and 3 newly installed permanent-magnet Halbach-array quadrupoles. The Halbach-array quadrupoles take significantly less space and are installed at locations that help with beam envelope control. Figure 7 shows the RMS beam envelope for  $3\sigma$  in both planes along with the corresponding physical aperture.

The MEBT line is equipped with several pieces of instrumentation for monitoring the beam, including 5 BPMs (each nested inside a quadrupole), an MEBT Allison scanner for measuring vertical Twiss parameters of the beam following the RFQ, a scanning wire to measure transverse beam profiles, a diamond detector capable of measuring single protons to study beam halo, a wall-current monitor, and two toroids to measure total beam current.

Beamline magnets include trim dipole packages, dipole bend magnets, and quadrupole magnets repurposed from the low-energy Electron Injector beamline build-out. There are also two multi-function frame magnets, acting as trims in both planes and as skew quadrupoles.

Beam current at the MEBT entrance is 3.7 mA due to relatively low transmission through the RFQ, which is on the order of 50 %. This is due to limitation of the current in

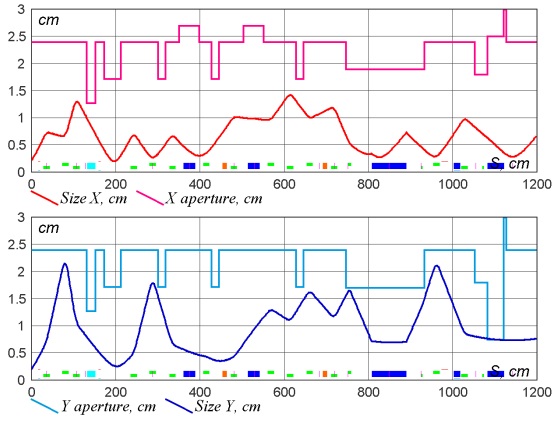


Figure 7: Beam envelope for  $3\sigma$  in the horizontal (top) and vertical (bottom) planes along with the corresponding aperture envelopes. The lattice starts from the exit of the RFQ and extends to IOTA, which starts around an azimuth of 1150 cm.

the first solenoid, which will be addressed by installation of new power supply and better cables. At the same time, transmission through the MEBT line is close to 100 %, thanks to good alignment and calibration of the magnets as seen in Fig. 8.

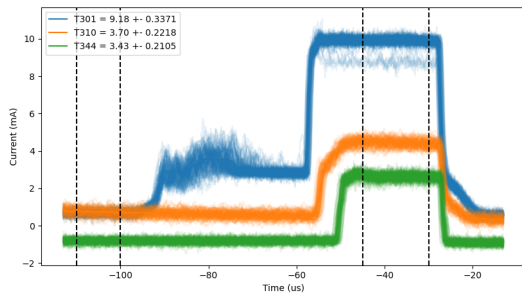


Figure 8: Beam current measured by toroids at different locations along IPI. The blue trace is for the toroid in LEBT, the orange trace is for the toroid right after RFQ and the green trace is for the toroid towards the end of the injection line.

## IOTA WITH PROTONS

Changing from electron to proton operations and the other way around requires manually swapping the leads of all unipolar power supplies that feed into IOTA's elements, which include the injection Lambertson, main dipoles, 39 quadrupoles, and several unipolar trims. The set points for the main elements were scaled down proportionally to the ratio of the momenta between 150 MeV/c electrons and 68.5 MeV/c protons. Another necessary modification involves changing kicker pulse length between roughly 100 ns for electrons to about 1700 ns for protons using different lengths of the pulse-forming coaxial cables.

Figure 9 shows injected beam envelopes in IOTA. The injected beam enters the ring through a horizontal Lambertson magnet. After exiting it, the beam is centered in the

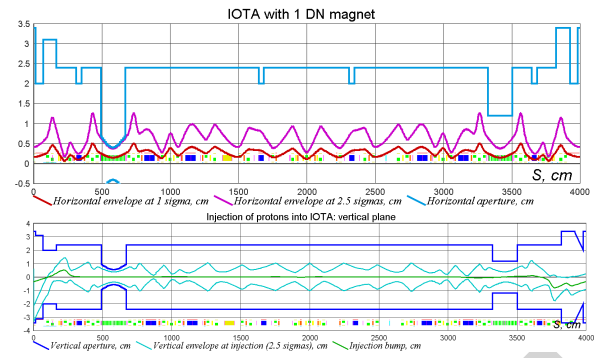


Figure 9: Injected beam envelopes for  $2.5\sigma$  in the horizontal (top) and vertical (bottom) planes along with the corresponding aperture envelopes. Injection happens from below near the beginning of the lattice.

horizontal plane and comes from below. Vertical kickers set the beam on a closed orbit shortly after that.

IOTA beam diagnostics consist of 21 button BPMs optimized for electron operations, 3 sets of striplines, a direct-current current transformer (DCCT), a wall current monitor (WCM), and 8 synchrotron light stations that are only applicable in electron mode of operations. The injected beam has a quickly decohering modulation at 325 MHz, which was originally planned to be used as the base frequency for the BPM signals, but it was shown in simulations [10] and in practice that the decoherence happens too quickly and the signal is too small for coordinate measurements. It was still practical to observe the residual modulation at the end of the first turn in IOTA in order to tune the amplitude and phase of the buncher cavity.

To measure coordinates with the BPMs, a 30.25 MHz cavity is activated to form bunches at the 55th harmonic of the revolution frequency. This regime allows both turn-by-turn measurements and a closed-orbit mode in which the coordinates are averaged over long time windows. The main limitation of this method is that it takes about 200 turns to fully bunch the injected beam, and it is hard to measure coordinates and current during this period.

The beam capture was facilitated by good ring alignment and element calibrations established during the electron runs. At present, only the DCCT can provide calibrated current measurements of the injected beam, and it is limited by a bandwidth on the order of 1 kHz, which does not allow resolution during the initial turns. The maximum current detected with the DCCT was on the order of 0.6–0.7 mA, which is about 10 times smaller than the TDR value. At the same time, detailed simulations [11] of the proton beam dynamics suggest that extremely strong space-charge forces will result in quick losses during the first thousand turns, and thus it is too early to draw final conclusions.

At 0.3 mA, the proton beam lifetime is about 18 seconds (Fig. 10). Vacuum levels around IOTA are in the low  $10^{-10}$  Torr range. At this level, the lifetime expected from scattering on the residual gas atoms is significantly longer than the measured values. There are two main rea-

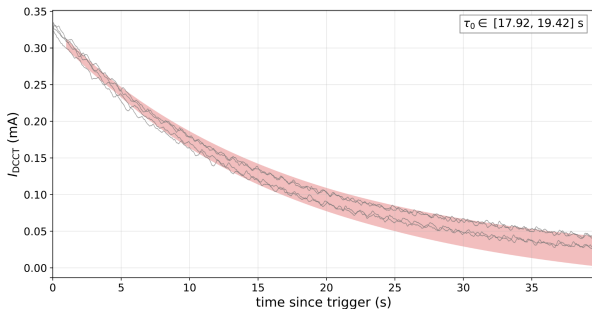


Figure 10: Stored proton current over time.

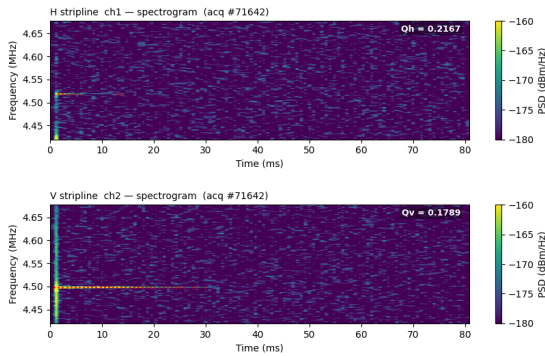


Figure 11: Betatron tunes measured at injection.

sions considered for the relatively short lifetime: intrabeam scattering and space-charge forces.

One set of striplines is used to measure betatron tunes by detecting the coherent signal from post-injection residual oscillations. The same method can be used with stored beam, with oscillations initiated by kickers at various amplitudes. The signal processing chain consists of a broadband 180-degree hybrid for creating the difference signal between opposite striplines, followed by a high-pass filter for excluding the fundamental harmonic and various sources of noise. In Fig. 11, we demonstrate the use of the upper betatron sidebands corresponding to the 8th revolution harmonic to measure the tunes.

## FUTURE PLANS

The remaining weeks of the current run will be used to finalize commissioning of the existing beam diagnostics, to match the MEBT line with the IOTA lattice, and to tune the IOTA lattice using the LOCO technique.

The upcoming summer shutdown will be used to install several essential IOTA upgrades that will boost the research capabilities in the proton mode. The most notable upgrade will be installation of horizontal and vertical ionization profile monitors (IPMs) [12]. These are devices that can measure transverse proton beam profiles with turn-by-turn resolution by collecting ions formed by the beam ionizing residual gas. Another important parameter that can be measured effectively with IPMs is the total beam current in turn-by-turn mode, for any shape of the longitudinal distribution. The DCCT also measures the total beam current, but its response time is on the order of a few hundred turns, which is not

enough to see very important beam dynamics during the first turns.

A chamber with two ceramic breaks is scheduled to be installed during the shutdown, which will allow a dual-frequency mode of operation of IOTA's wide-band RF cavity, with 30 MHz and 2.19 MHz options. Together with a high-power RF source, it will enable experiments on advanced manipulations of the longitudinal phase space.

The main objective of the IOTA experiments is to inform PIP-2 era solutions through cross-checking simulations with experimental data and testing controls solutions, including virtual accelerators and advanced AI/ML concepts. Among the immediate interests are studies aimed at understanding the benefits and constraints of various integrable lattices. One of the limitations of the presently installed Danilov-Nagitsev magnet is its small aperture. Therefore, a new insert with an opening about 50% larger was made; it is undergoing careful magnetic and mechanical characterization and is planned to be installed during the upcoming shutdown.

The main research thrusts and the corresponding type of beams are:

- Demonstration of integrable optics with special nonlinear magnets (e, p)
  - Thin radial kick of the McMillan type
  - Axially symmetric kick in a constant beta function
- Space-charge compensation with electron lenses (p)
- Space-charge compensation with electron columns (p)
- Optical stochastic cooling (e)
- Single electron studies (e)
- Electron cooling (p)
  - Electron cooling of protons
  - Diagnostics through recombination
  - Electron cooling and nonlinear integrable optics

## ACKNOWLEDGEMENTS

We would like to acknowledge and thank all those who have worked so hard to make the IPI, the IOTA ring, and the Electron Injector beamline a reality, both within the FAST facility departments and across the various organizations at Fermilab.

## REFERENCES

- [1] S. Antipov *et al.*, “IOTA (Integrable Optics Test Accelerator): facility and experimental beam physics program”, *J. Instrum.*, vol. 12, no. 03, T03002–T03002, Mar. 2017. [doi:10.1088/1748-0221/12/03/t03002](https://doi.org/10.1088/1748-0221/12/03/t03002)
- [2] M. Church *et al.*, “Proposal for an accelerator R&D user facility at Fermilab's Advanced Superconducting Test Accelerator (ASTA)”, Fermilab, Batavia, IL, USA, Rep. FERMILAB-TM-2568, Oct. 2013. [doi:10.2172/1422196](https://doi.org/10.2172/1422196)
- [3] W. Tan, “Characterization of the proton ion source beam for the high intensity neutrino source at Fermilab”, Ph.D. thesis, Indiana University, Bloomington, IN, USA, 2010.

- [4] R. D'Arcy, M. Alvarez, J. Gaynier, L. Prost, V. Scarpine, and A. Shemyakin, "Characterisation of the pxie allison-type emittance scanner", *Nucl. Instrum. Methods Phys. Res. A*, vol. 815, pp. 7–17, 2016.  
[doi:10.1016/j.nima.2016.01.039](https://doi.org/10.1016/j.nima.2016.01.039)
- [5] G. V. Romanov and A. Lunin, "Complete RF design of the HINS RFQ with CST MWS and HFSS", in *Proc. ICAP'09*, San Francisco, CA, USA, Aug.–Sep. 2009, pp. 340–342.
- [6] P. N. Ostroumov, V. N. Aseev, and A. A. Kolomiets, "Application of a new procedure for design of 325 MHz RFQ", *J. Instrum.*, vol. 1, P04002, Jan. 2006.  
[doi:10.1088/1748-0221/1/04/P04002](https://doi.org/10.1088/1748-0221/1/04/P04002)
- [7] R. C. Webber *et al.*, "Experiences with the Fermilab HINS 325 MHz RFQ", in *Proc. LINAC'10*, Tsukuba, Japan, Sep. 2010, pp. 515–517.
- [8] "TraceWin simulation package", <http://irfu.cea.fr/Sacm/logiciels/>,
- [9] G. Romanov *et al.*, "CW room-temperature bunching cavity for the project X MEBT", in *Proc. PAC'11*, New York, NY, USA, Mar.–Apr. 2011, pp. 1900–1902.
- [10] J. Wieland and A. Romanov, "Injection simulations of space charge dominated proton beams in IOTA", in *Proc. IPAC'25*, Taipei, Taiwan, Jun. 2025, pp. 995–998.  
[doi:10.18429/JACoW-IPAC2025-TUPB020](https://doi.org/10.18429/JACoW-IPAC2025-TUPB020)
- [11] N. Banerjee, A. Romanov, G. Stancari, and M. Wallbank, "Proton dynamics scenarios in the Integrable Optics Test Accelerator (IOTA) at Fermilab", *J. Instrum.*, vol. 21, no. 04, T04001, Apr. 2026.  
[doi:10.1088/1748-0221/21/04/T04001](https://doi.org/10.1088/1748-0221/21/04/T04001)
- [12] H. Piekarz, A. Romanov, V. Shiltsev, and R. Thurman-Keup, "Ionization profile monitors for the IOTA proton beam", *J. Instrum.*, vol. 20, no. 10, T10007, Oct. 2025.  
[doi:10.1088/1748-0221/20/10/T10007](https://doi.org/10.1088/1748-0221/20/10/T10007)